OPEN ACCESS INTERNATIONAL JOURNAL OF SCIENCE & ENGINEERING

EFFECT OF DL-MALIC ACID ON STRUCTURAL, OPTICAL, MECHANICAL AND NLO PROPERTIES OF NINHYDRIN SINGLE CRYSTALS

K. Lilly Mary Eucharista[1], C. Krishnan[2] , P.Selvarajan[3]

Department of Physics, Sri Meenakshi Govt.Arts College for Women (Autonomous), Madurai -625 002. Tamil Nadu, India[1]

Department of Physics, Arignar Anna College, Aralvoymoli-629301,Tamil Nadu, India[2]

Department of Physics, Aditanar College of Arts and Science, Tiruchendur-628216, Tamil Nadu, India.[3]

lilly.mary@ymail.com[1]

Abstract: **Single crystal of linear optical DL-Malic acid ninhydrin (DLMN) has been grown in the laboratory by slow evaporation method for the first time. The grown crystal was subjected to single crystal X-ray diffraction analysis to confirm the crystal structure and it was found to be monoclinic. Structural characterizations of the grown crystals were carried out by powder crystal X-ray diffraction method. The presence of the functional groups and modes of vibrations were identified by FTIR spectroscopy recorded in the range 4000-400cm^{-1}. The optical absorption studies show that the crystal is transparent in the entire visible region with a cut off wavelength of 272 nm. The optical band gap was calculated to be 4.565 eV. With the help of optical data, the optical constants were calculated. The mechanical strength of the grown crystal was estimated by the Vickers hardness test. The second harmonic generation efficiency was measured by powder Kurtz method, which is 2.4 times that of KDP. The encouraging results show that the DLMN crystals have great potential applications in optical devices**

Keywords *– Single Crystal, FTIR analysis, Mechanical properties, Organic crystals, SHG, X-ray diffraction*

----------∴∴∴----------

I INTRODUCTION

In recent years the search for new organic materials with high optical nonlinearity is an important area due to their practical applications such as optical communication, optical computing, laser remote sensing and so forth [1] [2] [3]. Ninhydrin is an organic material, with high melting point. It is an important analytical tool in various fields including soil biology, chemistry, agriculture, medicine and so on. R.C. Medrud reported the crystal structure of ninhydrin [4] [5]. T. Prasanyaa et al., reported the antimicrobial activity and second harmonic studies on organic non - Centro symmetric pure and doped (cu2+, cd2+ ions) ninhydrin single crystals [6]. A.Ponchitra et al., reported the effect of $Zn^{2+,}$ Ni^{2+} Substitution on Structural, Optical and Mechanical Properties of Ninhydrin Crystals [7]. Some doped transition metal ions influence the habit modification and growth kinetics. No literature was found with the effect of organic acid on ninhydrin single crystal. Hence we concentrate our work on the effect of DL- malic acid on growth and characterization of ninhydrin.

II EXPERIMENTAL METHOD

X-ray diffraction (SCXRD) studies carried out by Enraf Nonius CAD4 single crystal X-ray diffractometer with CuKα (λ=1.5406 Å) radiation. The grown DLMN crystal has been crushed into fine powder and subjected to powder XRD study using a XPert Pro Powder X-ray diffractometer with CuKα radiation (λ=1.5406Å). The sample was scanned in the 2θ values ranging from 10^o to 80^o. The optical transmission spectrum of DLMN crystal was recorded using a UV-Vis-NIR spectrophotometer (Lambda 35 model) from 190 to 1100 nm. A Perkin Elmer FTIR spectrometer was used for IR spectral measurements. The sample was prepared by the KBr pellet tecnique and the spectrum was rcorded in the range of 4000-400 cm^{-1}. The DLMN crystal was tested for the microhardness property using a Vickers microhardness tester. The SHG test for the grown DLMN crystals was performed by the powder technique of Kurtz and Perry.

III RESULTS AND DISCUSSION

3.1 Synthesis and solubility

The starting materials were of analytical reagent, and the synthesis and growth process were carried out in aqueous solution. DLMN compound was synthesized by taking DL-Malic acid and Ninhydrin in a 1:1 stoichiometric ratio. The calculated amounts of DL-Malic acid and Ninhydrin were dissolved in the deionized water. Purity of the synthesized salt was improved by successive recrystallization. Optically transparent and defect free crystals of DLMN obtained by slow evaporation technique. Solubility is defined as the amount of solute in grams present in 100 ml of saturated solution at a particular temperature and provides a driving force for both nucleation and crystal growth. The solubility study was carried out for the DLMN salt in double distilled water by gravimetrical method [8]. Initially, solubility was determined at 30^{o}C by dissolving the solute in 25 ml of double distilled water maintained at a constant temperature using magnetic stirrer. DLMN salt was added in small amount at successive stages and then the solute was added till a small precipitate was formed. This gave a confirmation of the super saturated condition. Then the 5 ml of the saturated solution was pipetted out and taken into a petri dish of known weight and it was heated till the solvent was evaporated. The amount of the salt present in 5 ml of the solution was measured by subtracting the empty petri dish's weight. From the above value, the amount of the salt present in 100 ml of the solution was found out. The same procedure was followed for the temperatures 30, 35, 40, 45 and 50^{o}C. The solubility diagram of the DLMN salt is displayed in Figureure1.

3.2. Crystal growth

Based on the solubility data the title compound was synthesized by dissolving high purity DL-Malic acid and Ninhydrin in distilled water in the ratio of 1:1. The resulting solution was stirred well of about two hours and filtered to allow crystallization by slow solvent evaporation method at room temperature. Tiny single crystals (Figure2) were harvested after a span of 30 days with good quality.

3.3. X-ray diffraction analysis

Single crystal X-ray diffraction analysis reveals that DL- Malic acid Ninhydrin single crystal belongs to the monoclinic system. The calculated unit cell parameters for DLMN crystal are a = 11.336(8) Å, b = 6.022(4) Å, c = 5.745(5) Å, α = γ = 90˚, β = 98.64˚ and V = 387.74 Å^3 and the unit cell parameters for pure ninhydrin single crystal are a = 11.2789 Å, b = 6.085 Å, c = 5.778 Å, α = γ = 90˚, β = 99.3˚ and V = 396.82 Å^3 [9]. Also, the powder XRD pattern of the grown DLMN single crystal was recorded and indexed is shown in Figure 3. The sharp Bragg peaks of powder XRD pattern were indexed using the TREOR software package following the procedure of Lipson and Steeple [10]. Specific well-defined peaks at 2θ values indicate high crystallinity of the grown DLMN crystal.

3.4. FTIR Analysis:

The FTIR spectrum was recorded for the grown crystal in the range 400–4000 cm^{-1}at room temperature. The recorded FTIR spectrum of DLMN is shown in Figure 4. The FTIR spectral analysis was carried out to identify the functional groups present in the compound. The strong absorption peak at 3187 symmetric stretching [5] is due to aromatic O–H stretching. The peak at 3089.08 cm^{-1} belongs to the aromatic C-H stretching for the pure and grown DLMN single crystal. The recorded peaks at 1761.42 cm^{-1} and 1712.01 cm^{-1} are due to carbonyl (C= O) stretching [11]. A medium intense peak observed at 1585.17 cm^{-1} is attributed to aromatic ring vibration [11].The skeletal vibration of aromatic ring is observed at 1585.17 cm^{-1} in DLMN crystal. The peaks at 1297.73 cm^{-1}, 1178.31 cm^{-1}, 1079.47 cm^{-1}, are all due to in plane bending modes of aromatic C-H bonds. The out of plane aromatic C-H bond is observed at741.79 cm^{-1} [12]. The peaks observed at 1374.33 cm^{-1} , 938.64 cm^{-1} , 622.37 cm^{-1} are due to C-H rock, O–H bend (carboxylic acid), C–H bend respectively .This observed shift in vibrational frequency is an evidence for the formation of the title compound

3.5. UV-Visible spectral analysis

The optical transmittance property gives important information on materials, particularly the optical transparency window, which is used in linear and nonlinear applications. The optical transmission spectrum for the grown crystal was recorded in the range of 190–1100 nm, and the obtained spectrum is shown in Figure5. The spectrum's characteristics can be attributed to the promotion of electrons in the σ-, π- and n-orbitals from the ground state to higher states. The spectrum reveals that the grown DLMN crystal has a superior optical transmittance in the high visible area and shows no remarkable absorption in the visible region. This is an important property for nonlinear optical applications. The lower cutoff wavelength is as low as 270 nm due to the π–π* conversion in this crystalline material [13].

The transmittance of the DLMN crystals is approximately 75%. The transmission extends from 270 to 1100 nm, which suggests that these materials may be used in optical window applications. The band gap energy was calculated from the graph between hν and $(\alpha h\nu)^2$ by extrapolating the linear portion of the curve to zero absorption as shown in Figure 6. Here α is the absorption coefficient and hν is the photon energy. The band gap energy estimated is about 4.565 eV for the DLMN single crystal. The band gap is found to be greater than the reported value 2.5 eV [5] which attribute the effect of DL malic acid. The wide

optical band gap of the grown DLMN crystal is suggesting its suitability for optoelectronics applications.

3.5.1. Determination of optical constants

The optical acrimony of materials is essential to determine its performance in opto-electronic devices. Measurement of the refractive index is vital for frequency doubling experiments and in appraisement of optical parameters when employing NLO crystals. The optical properties may be too closely relevant to the material's atomic structure, electronic band structure and electrical properties. The diverse optical constants were also calculated using the following theoretical formulae [14]. Extinction coefficient (K) can be determined from the equation as follows,

$$K = \lambda\alpha / 4\pi \quad (1)$$

Where, λ is the wavelength of the ultraviolet radiation. The reflectance (R) in terms of absorption coefficient and refractive index (n) can be written as [15],

$$R = 1 \pm \frac{\sqrt{(1-exp(-\alpha t)+exp(\alpha t)}}{1+\exp(-\alpha t)} \quad (2)$$

$$n = - \frac{(R+1) \pm \sqrt{3R2 + 10R - 3}}{2(R+1)} \quad (3)$$

K as a function of photon energy and reflectance and refractive index as function of wavelength are plotted in the Figures. 7, 8 and 9. From these plots, it is known that the refractive index decreases with the increase of wavelength. The calculated refractive index (n) is 1.845 for the DLMN crystal at 270 nm. High optical transparency, low absorbance, low reflectance and low refractive index of DLMN in the UV-visible region concludes that the material as a vital one for antireflection coating in solar thermal devices and NLO applications.

The photonic response of optical conductivity (σ_{op}) of the material when irradiated with light is relevant to the refractive index (n) and the speed of light (c) as follows

$$\sigma_{op} = \frac{\alpha nc}{4\pi} \quad (4)$$

and also the electrical conductivity is correlated to the optical conductivity of the DLMN crystal as follows,

$$\sigma_e = \frac{2\lambda\sigma op}{\alpha} \quad (5)$$

Figure10 depict that the optical conductivity increases with photon energy, having high magnitude (10^{10} $(\Omega\ m)^{-1}$) and electrical conductivity (10^{8} $(\Omega\ m)^{-1}$) supports semiconducting nature of the material . The low extinction value (10^{-5}) suggests that this material make more germane for device applications in computing ultrafast optical data . The electric susceptibility (χc) is closely connected to optical constants given by [16],

$$\varepsilon_r = \varepsilon_0 + 4\pi\chi_c = n^2 - K^2 \quad (6)$$

$$\chi_c = \frac{n2 - K2 - \varepsilon 0}{4\pi} \quad (7)$$

where ε0 is the dielectric constant in absence of any contribution from free carriers. The real part (ε_r) and imaginary part (ε_i) of the dielectric constants can be evaluated using the relations,

$$\varepsilon_r = n^2 - K^2 \text{ and } \varepsilon_i = 2nK \quad (8)$$

The real and imaginary parts of the dielectric constant of the grown crystal were determined and shown in Figureure 11. From the graph, both real and imaginary part of dielectric constant increases with increase of photon energy. Both dielectric constants are maximum at 6.53 eV photon energy. The lower value of dielectric constant with wide band gap of DLMN crystal suggests the suitability of optoelectronic devices.

3.6. Vickers microhardness test

The mechanical characterization of DLMN crystal was made by Vickers microhardness tests at room temperature. Hardness of the material carries information about the strength, molecular bindings, yield strength and elastic stiffness constant [17]. The mechanical strength of the materials plays a significant key role in device fabrication. The hardness measurement on a crystal provides information about the elastic, plastic, viscous and fracture properties. The Vickers microhardness measurement convicts the mechanical property of grown DLMN crystal. The microhardness test was carried out at room temperature and loads of various magnitudes such as 25, 50 and 100 g were applied. The Vickers microhardness number is calculated using the expression using the standard formula,

$$H_v = 1.8544 \times P/d^2 \quad (9)$$

where P is the applied load in kg, d is the diagonal length of the indented impression in mm and H_v is Vickers microhardness number in kg/mm^2 [18]. Figure12. shows the variation of hardness number (H_v) as an event of applied load ranging from 25 – 100g for DLMN crystal. According to the normal Indentation Size Effect (ISE), the micro hardness number of a crystal decreases with increasing load and according to the Reverse Indentation Size Effect (RISE), the hardness number of a crystal increases with increasing load [19][20]. From the plot, it is found that the hardness number increases with increase in load up to 100 g, further increase in load create the cracks on the surface of the crystal due to the release of internal stresses produced by indentation.

. The n value was calculated using Meyer's law is given by following relation [21]

$$P = k\ d^n \quad (10)$$

$$\text{Log } P = \log k + n \log d \quad (11)$$

where k is the material constant and 'n' is the Meyer's index. In order to find the value of 'n', a graph is plotted for log P against log d (Figure 13) which gives a straight line. From the slope of the line the Meyer's index number 'n' was calculated to be 2.486. For the regular ISE behavior we have n< 2. When n >2, there is a reverse ISE behavior. This is in good consent with the experimental data and thus confirms the reverse ISE behavior. According to Onitsch, 'n' should lie between 1 and 1.6 for harder materials and above 1.6 for softer material. Thus DLMN belongs to the soft material category.

3.6.1. Elastic stiffness constant

The elastic stiffness constant (C_{11}) was calculated using Wooster's empirical formula which gives an idea about the tightness of bonding between neighboring atoms

$$C_{11} = Hv^{7/4} \quad (12)$$

The calculated stiffness constant for loads 25, 50 and 100 g are 14.983 x 10^{12}, 26.480 x 10^{12} and 86.916 x 10^{12} Pa respectively. The elastic stiffness constant (C_{11}) gives an opinion of tightness of bonding between neighboring atoms. A graph is plotted between load P vs. stiffness constant C_{11} and is represented in Figure 14. From the graph it clears that the stiffness constant increases with increase of load. The high value of stiffness constant C_{11} reveal that the binding forces between the ions are quite strong.

3.6.2. Fracture Mechanics

The resistance to fracture indicates the toughness of any material. Fracture toughness (K_c) determines how much fracture stress is applied under uniform loading and is an important parameter for the selection of materials for device applications where the load exceeds the limit or yield point. Fracture toughness provides the most reasonable estimation of the fracture resistance of brittle materials. The crack lengths (c) were measured from centers of the indentation to the tip of the crack.

$$K_c = P/\beta_0 c^{3/2} \quad (13)$$

where β0 is a constant that depends upon the indentation geometry. For Vickers indenter β_0 is equal to 7. For the DLMN crystal the calculated K_c was 19.683 $Kgm^{-3/2}$.

3.6.3. Brittleness Index

Brittleness is an important property that affects the mechanical behavior of a material and gives an idea about the fracture induced in a material without any appreciable deformation. The value of brittleness index B is calculated using relation

$$B = H \sqrt{K_c} \quad (14)$$

The calculated values of fracture toughness and hardness value for various loads are plotted in Figure15. The graph shows the linear relationship of the two parameters and the slope of this straight line gives the brittleness index of the sample. The brittleness index of DLMN crystal is estimated as 0.9716 × 10^3 $m^{-1/2}$. The low value of the brittleness index reveals the good dimensional stability of the grown crystal. The calculated stiffness constant C_{11}, yield strength σ_y and Vickers hardness values for different load range 25-100 g are compiled in Table 2.

3.7. Second Harmonic Efficiency

The second harmonic nonlinear optical property of the as grown DLMN crystal was examined through the Kurtz-Perry powder technique. The standard KDP crystal has been used as the reference material for the grown crystal. In this method powdered sample of randomly oriented crystalline particles were placed in between two glass slides. The sample was then subjected to the output of Q-switched Nd:YAG laser emitting a wavelength of 1064 nm with power of 1.2 mJ/pulse. The output SHG signal of 96 mV was obtained for the DLMN crystal. The KDP crystal gave an output of 40 mV for the same input signal. Thus it is evident that the SHG efficiency of the grown DLMN crystal is 2.4 times than that of the KDP crystal and is found to be greater than the reported value [7] and thus the crystal is suitable for nonlinear optical device fabrication.

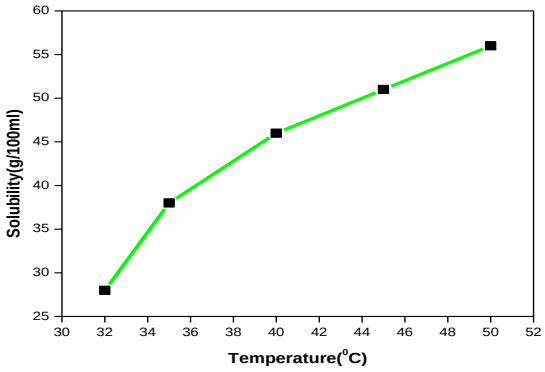

Figure 1 Solubility curve of DLMN crystal

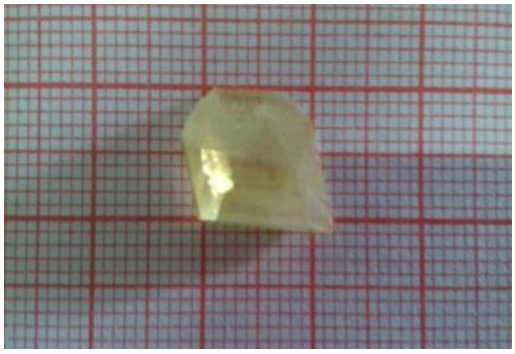

Figure 2 Photograph of the grown DLMN crystal

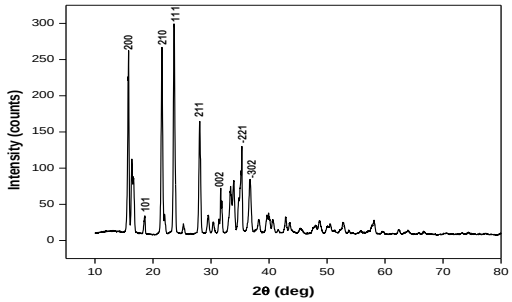

Figure 3 Powder X-ray diffraction pattern of DLMN crystal

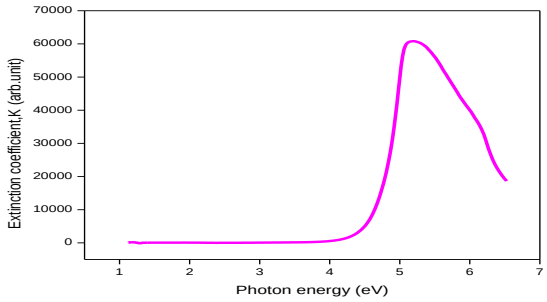

Figure 7 Plot of K vs. photon energy of DLMN crystal

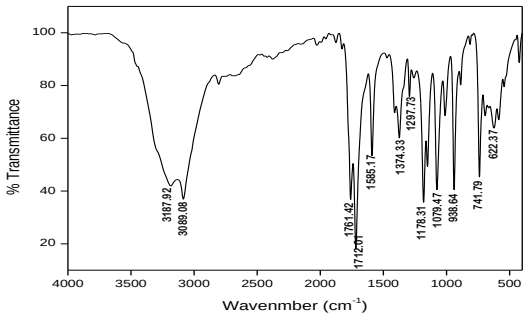

Figure 4 FTIR spectrum of DLMN single crystal

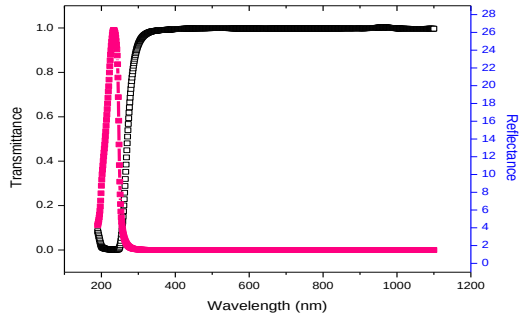

Figure 8 Plot of reflectance (R) and transmittance vs. wavelength of DLMN crystal

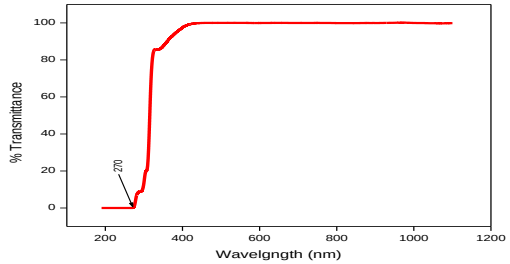

Figure 5 Transmittance spectrum of DLMN crystal

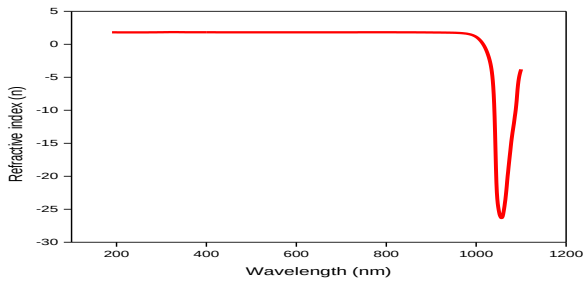

Figure 9 Variation of refractive index with wavelength of DLMN crystal

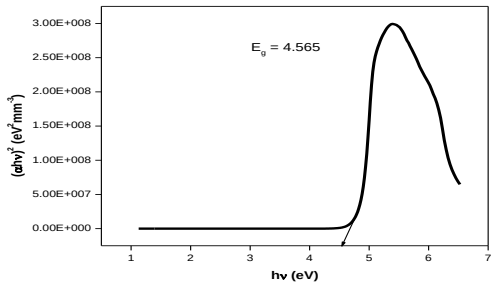

Figure 6 Band gap spectra of DLMN crystal

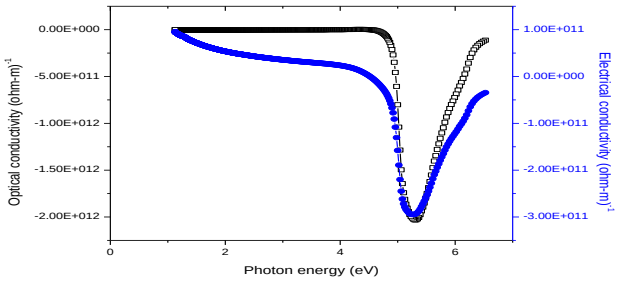

Figure 10 Variation of optical conductivity and electrical conductivity vs. photon energy of DLMN crystal

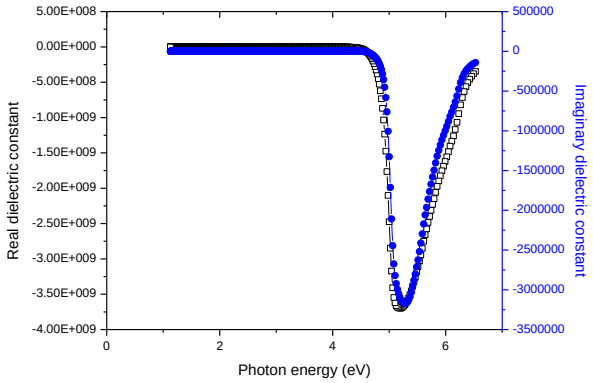

Figure 11 Variation of real and imaginary dielectric constant with photon energy of DLMN crystal

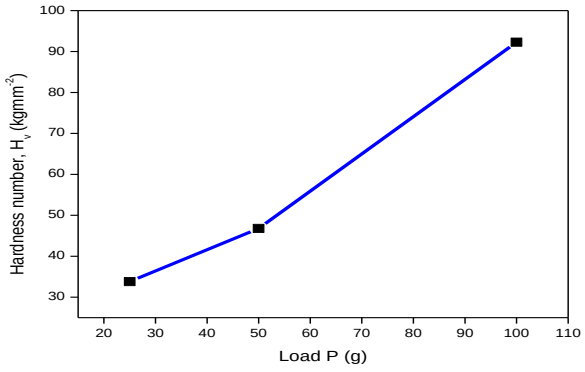

Figure 12 Variation of hardness number with load for DLMN crystal

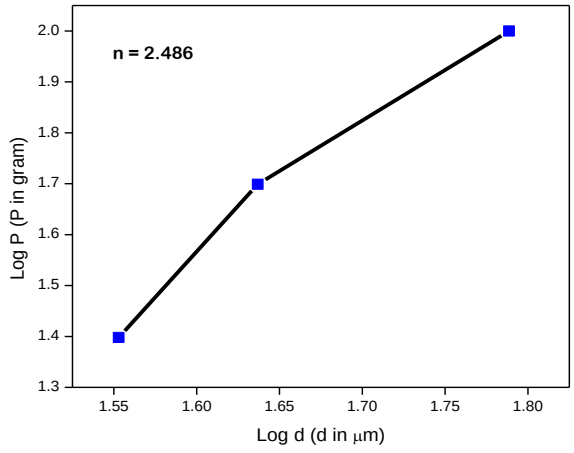

Figure 13 Plot of log (P) vs log (d) for DLMN crystal

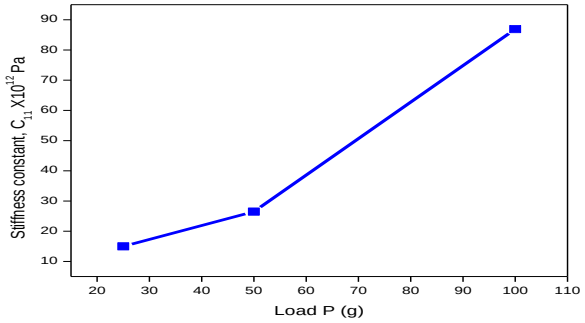

Figure 14 Plot of load P vs. Stiffness constant C_{11} for DLMN crystal

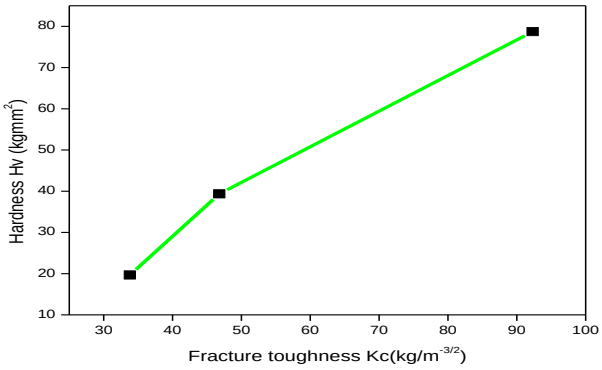

Figure 15 Plot of Kc vs. H_v of DLMN crystal

IV CONCLUSION

Single crystal of DL Malic acid Ninhydrin was successfully grown by slow evaporation technique. Single X-ray diffraction study confirms that lattice parameter values of the grown crystal are in good agreement with the reported values. From the single crystal X-ray diffraction study the lattice parameter values of the crystal were found to be *a* = 11.336(8) Å, *b* = 6.022(4) Å, *c* = 5.745(5) Å, α = γ = 90˚, β = 98.64˚ and *V* = 387.74 Å^3 and it is crystallized in monoclinic crystal system with the space group P_{21}. FT-IR studies confirm the presence of functional groups present in the crystal. Optical studies were carried out for the grown crystal and the crystal has wide transparency window between 190 nm – 1100 nm. Various optical constants were calculated and the optical band gap energy of the crystal is found to be 4.565 eV. The extinction coefficient (K) and reflectance depend on the photon energy and absorption coefficient. The refractive index of the material is found to be 1.845 at a wavelength of 270 nm. Optical conductivity is calculated from the UV - Vis absorbance value and the grown crystal possesses high electrical and optical conductivity.

Vickers hardness number is calculated as 2.486, so the material belongs to soft material category. The fracture toughness of the material is found to be 19.683 $Kgm^{-3/2}$. The B value is computed as 0.9716 x 10^3 $m^{-1/2}$. The value of C_{11} gives an idea of tightness of bonding between neighboring ions. The SHG efficiency of the grown DLMN crystal is 2.4 times than that of the KDP crystal and the DLMN crystal is suitable for nonlinear optical device fabrication.

REFERENCES

[1] C.K. Lakshmana Perumal, A. Arulchakkaravarthi, N.P. Rajesh, P. Santhana Raghavan, Y.C. Huang, M. Ichimura, P. Ramasamy, Journal of Crystal Growth, 240(1-2), 2002, 212-217.

[2] F.Zermike, J.Midwinte, Applied Nonlinear Optics, Wiley, New York (1973).

[3] J.Zyss. J. Mol. Electron. 1(18) (1985) 25-45.

[4] R.C. Medrud, Acta Crystallographica B, 25(2), 1969, 213-220.

[5] T. Uma devi, N. Lawrence, R. Ramesh babu, K. Ramamurthi and G. Bhagavannarayana, Spectrochimica Acta A: Molecular and biomolecular Spectroscopy, 71(5), 2009, 1667-1672.

[6] T. Prasanyaa, V. Jyaramakrishnan, M. Haris, Spectrochimica Acta Part A: Molecular and biomolecular Spectroscopy, 104, 2013, 110-113.

[7] A.Ponchitra, K.Balasubramanian, International Journal of Scientific & Engineering Research,(2017) , 8, 55-58.

[8] W.S. Wang, K. Sutter, Ch. Bosshard, Z. Pan, H. Arend,P. Gunter, G. Chapuis, F. Nicolo, Jpn. Journal ofApplied Physics, 27 (7), pp. 1138-1141, 1988

[9] N. Vijayan, J. Philip, D. Haranath, Brijesh Rathi, G. Bhagavannarayana, S.K. Halder, N. Roy, M.S. Jayalakshmy, Sunil Verma, Spectrochimica Acta Part A: Molecular and Biomolecular Spectroscopy 122 (2014) 309–314

[10] H.Lipson, H.Steeple, Interpretation of X-Ray Powder Diffraction patterns, fifth ed. Macmillan, New York, 1970.

[11] R. J. Dyer, Applications of Absorption Spectroscopy of Organic Compounds, Prentice Hall, New Delhi, India, 1994.

[12] K. Biemann, Tables of Spectral Data for Structure Determination of Organic Compounds, Springer, Berlin, Germany, 1989.

[13] R.S. Sreenivasan, N.Kangathara, G. Ezhamani, N.G. Renganathan and G. Anbalagan, Journal of spectroscopy, (2013)

[14] P.V. Dhanaraj, T. Sudan, N.P. Rajesh, Curr. Appl. Phys. 10 (2010) 1349-1353.

[15] R. Surekha, R. Gunaseelan, P. Sagayaraj, K. Ambujam, The Roy. Soc. Chem. 16 (2014) 7979-7989.

[16] W.J. Jones, W.J. Orville-Thomas, Trans. Faraday Soc. 55 (1959) 203-210

[17] K. Li, X. Wang, D. Xue, Mater. Focus 1(2012) 142-148.

[18] Susmita Karan, S.P. Sen Gupta, Mater. Sci. Eng. A 398 (2005) 198.

[19] J.Mary Linet, S.Jerome Das, Physica B 405 (2010) 3955 - 3959.

[20] B.Helina, P.Selvarajan, A.S.J.Lucia Rose, Phys.Scripta, 85 **(**2012) 055803 - 055808.

[21] K. Sangwal, B. Surowska, P. Blaziak, J. Mater. Chem. Phys. 80 (2003) 428- 437